Contribution from the Chemical Research Institute of Non-Aqueous Solutions, Tohoku University, Katahira, Sendai 980, Japan

[5,10,15,20-Tetrakis(1-methylpyridinium-2-, -3-, and -4-yl)porphinato]iron Complexes As Seen by Electronic Absorption, Magnetic Circular Dichroism, and Electron Paramagnetic Resonance Spectroscopy

NAGAO KOBAYASHI

Received October 18, 1984

Magnetic circular dichroism (MCD) and electronic absorption spectra are reported for [5,10,15,20-tetrakis(1-methylpyridinium-2- and -3-yl)porphinato]iron, FeT2MP and FeT3MP, in the near-UV to near-IR regions. Electron paramagnetic resonance (EPR) spectra are also reported for the Fe^{III}T2MP, Fe^{III}T3MP, and Fe^{III}T4MP ([5,10,15,20-tetrakis(1-methylpyridinium-4-yl)porphinato]iron(III)) species. In each FeTMP, three ferric and two ferrous species are sufficient to explain the results at all pH values. Proton equilibria exist between the three Fe^{III}T2MP or Fe^{III}T3MP monomers with pK_a values around 5-6 and 11-12. After electrochemical reduction, an equilibrium is observed between the two Fe^{II}T2MP or Fe^{II}T3MP monomers with a pK_a of around 11-12. The species are in high-spin states except at high pH; low-spin states exist for Fe^{III}T3MP and Fe^{III}T4MP at pH >13 and for Fe^{III}T2MP and Fe^{II}TMPs at pH >12. The effective symmetry of iron increases approximately in the sequence of FeT2MP, FeT3MP, and FeT4MP; i.e. the farther the pyridinium group from the porphyrin plane, the more symmetric iron becomes. The electronic structures of the coordination spheres of these structural isomers are discussed in the context of previously studied iron porphyrins and hemes.

Introduction

As one of the most important representatives of water-soluble porphyrins, the iron complex of 5,10,15,20-tetrakis(1-methylpyridinium-4-yl)porphine, FeT4MP, has been widely used in both spectroscopic[1,2] and electrochemical[3] studies. However, there has been little research[4] on the structural isomers of FeT4MP, i.e. FeT2MP and FeT3MP (Figure 1). Recently, we reported detailed MCD studies on FeT4MP[5] with discussion of the proton equilibria and of the porphyrin electronic structure of the coordination sphere. Three monomeric iron(III) species and two monomeric iron(II) species were recognized for FeT4MP. If there are 5 states for FeT2MP and FeT3MP, it would be possible to compare the results of all 15 states among the 3 structural isomers. In this work, we present the results of FeT2MP and FeT3MP as seen by MCD, EPR, and electronic absorption spectroscopy and of FeT4MP as seen by EPR. As will be shown, the difference in the position of the pyridinium group affected several factors.

Experimental Section

(i) Materials. Chemicals were commercially available guaranteed reagents and were used without further purifications. Fe^{III}T2MP(Cl) and Fe^{III}T3MP(Cl) were prepared by the method that Fleischer used to synthesize FeT4MP(Cl).[1a] 5,10,15,20-Tetrapyridylporphyrins were refluxed for 1 h with 2,3-dichloro-5,6-dicyanoquinone in benzene-tetrahydrofuran (4:1 v/v) prior to methylation to eliminate chlorine impurities. The ratios of C:N:Fe were experimentally determined to be 44:7.9:0.98 for Fe^{III}T2MP(Cl) and 44:7.9:0.99 for Fe^{III}T3MP(Cl) as compared to the theoretical value of 44:8:1. Electrochemical reduction to give Fe^{II}T2MP and Fe^{II}T3MP was performed with an optically transparent thin-layer electrode (OTTLE), at a potential of -0.7 V[4c] vs. a saturated calomel electrode (SCE) maintained by a potentiostat that was built according to the literature.[6] For the pH-variation experiments, the FeTMPs were dissolved in a 0.05 M (1 M = 1 mol dm^{-3}) Na_2SO_4 solution. The pH was adjusted with concentrated H_2SO_4 or NaOH solutions. However, for highly basic (pH >12) solutions, the iron porphyrins were first dissolved in dilute NaOH solution and then Na_2SO_4 was added to produce a solution with ionic strength between 0.15 and 0.20. Also, 0.05 M H_2SO_4 and 0.5 and 1 M NaOH solutions were used. The porphyrins were first dissolved in deuterated water, and the pD was adjusted with concentrated DCl and NaOD solutions for measurements above 1000 nm.

Small rectangular OTTLEs with a gold or platinum minigrid as the working electrode were constructed[7] to fit into the holders of the absorption and MCD apparatus.

(ii) Measurements. Absorption spectra were measured with a JASCO Uvidec-1 spectrophotometer. MCD spectra were recorded by use of JASCO J-500 and J-200 spectrodichrometers equipped with a data processor and an electromagnet that produced magnetic fields up to 1.17 T (1 T = 10000 G), with parallel and then antiparallel fields. The field magnitude was expressed in terms of molar ellipticity per tesla, $[\theta]_M/10^4$ deg mol^{-1} dm^3 cm^{-1} T^{-1}. Cells with path lengths of 1 and 10 mm were used. The path lengths of the OTTLEs were determined to be 0.29 and 1.04 mm by measuring and comparing the absorbance of the Soret band of a freshly prepared Fe^{III}T2MP solution whose concentration had been predetermined in a calibrated 1-cm cuvette. Experiments using OTTLEs were conducted under a nitrogen atmosphere. EPR spectra were recorded at 77 K with a JEOL FE3AX spectrometer with 100-kHz field modulation. The magnetic field was measured by proton resonance, and the microwave frequency was calibrated by using MnO_2 as standard (g = 2.006 54). A Hitachi-Horiba M-7 pH meter was used to determine the pH.

Results and Discussion

(i) Proton Equilibria. (a) Proton Equilibria between Fe^{III}TMP Species. Figure 2 shows the electronic absorption spectra in the Soret region of Fe^{III}T2MP (top) and Fe^{III}T3MP (bottom) at pH values of 1-7 (left side) and 7-13.7 (right side). At pH values above 10, the spectra changed gradually; therefore, the spectra were obtained immediately after the preparation of each sample solution. The dependence of the absorbance on pH at several wavelengths (taken from data in Figure 2) is plotted in Figure 3. Three different species are indicated between pH 1 and 13.7 (Figure 3), and a set of two inflection points was observed for each Fe^{III}TMP (Figure 2). The positions of the inflection points were the same irrespective of the wavelength examined. Thus, two proton-transfer equilibria exist, one at pH 4-8 and the other at pH 10-14. In order to avoid the problem of monomer-dimer equilibrium, which makes analysis difficult, a Beer's law test was

(1) (a) Fleischer, E. B.; Hambright, P. *Inorg. Chem.* **1970**, *9*, 1757. (b) Pasternack, R. F.; Lee, H.; Malek, P.; Spencer, C. *J. Inorg. Nucl. Chem.* **1977**, *39*, 1865. (c) Pasternack, R. F.; Spiro, E. G. *J. Am. Chem. Soc.* **1978**, *100*, 968. (d) Larris, F. L.; Toppen, D. L. *Inorg. Chem.* **1978**, *17*, 71. (e) Goff, H.; Morgan, L. O. *Ibid.* **1976**, *15*, 3181. (f) Welnraub, D.; Peretz, P.; Faraggl, M. *J. Phys. Chem.* **1982**, *86*, 1839, 1842.

(2) (a) Forshey, P. A.; Kuwana, T. *Inorg. Chem.* **1981**, *20*, 693. (b) Kurihara, H.; Arifuku, F.; Ando, I.; Saita, M.; Nishimoto, R.; Ujimoto, K. *Bull. Chem. Soc. Jpn.* **1982**, *55*, 3515.

(3) (a) Kuwana, T.; Fujihira, M.; Sunakawa, K.; Osa, T. *J. Electroanal. Chem. Interfacial Electrochem.* **1978**, *88*, 299. (b) Kuwana, T.; Bettelheim, A. *Anal. Chem.* **1979**, *51*, 2257. (c) Kuwana, T.; Forshey, P. A. *Inorg. Chem.* **1983**, *22*, 699. (d) Kuwana, T.; Forshey, P. A.; Kobayashi, N.; Osa, T. *Adv. Chem. Ser.* **1982**, *No. 201*, 601. (e) Kobayashi, N.; Fujihira, M.; Sunakawa, K.; Osa, T. *J. Electroanal. Chem. Interfacial Electrochem.* **1979**, *101*, 269.

(4) There are, however, a few studies on nonmetalated or cadmium- or zinc-inserted T2MP and T3MP, e.g.: (a) Hambright, P.; Gore, T.; Burton, M. *Inorg. Chem.* **1976**, *15*, 2314. (b) Shamim, A.; Hambright, P. *Ibid.* **1980**, *19*, 564. (c) Hambright, P. *Ibid.* **1977**, *16*, 2987. (d) Torrens, M. A.; Straub, D. K.; Epstein, M. L. *J. Am. Chem. Soc.* **1972**, *94*, 4160 (concerned with the μ-oxo dimer of FeTMPs).

(5) Kobayashi, N.; Koshiyama, M.; Osa, T.; Kuwana, T. *Inorg. Chem.* **1983**, *22*, 3608.

(6) Kuwana, T.; Strojek, J. W. *Discuss. Faraday Soc.* **1968**, *45*, 134.

(7) DeAngelis, T. P.; Heineman, W. R. *J. Chem. Educ.* **1976**, *53*, 594. (b) Anderson, C. W.; Halsall, H. B.; Heineman, W. R. *Anal. Biochem.* **1979**, *93*, 366.

0020-1669/85/1324-3324$01.50/0

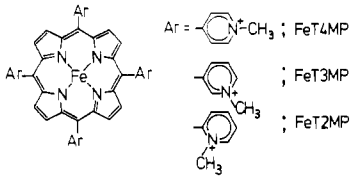

Figure 1. Structure of FeTMPs.

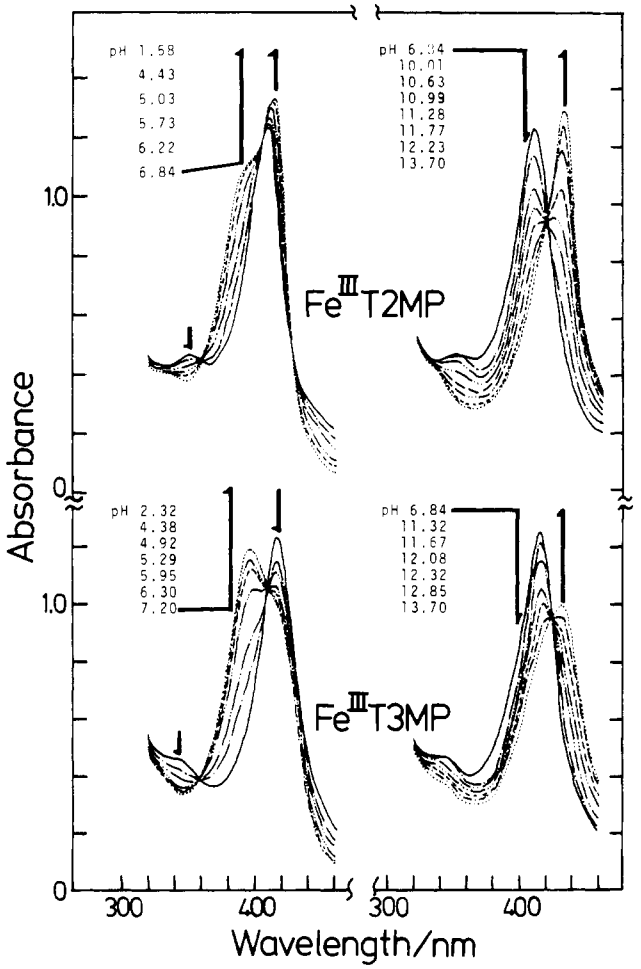

Figure 2. Soret absorption spectra of $Fe^{III}T2MP$ and $Fe^{III}T3MP$ aqueous solutions at various pHs ($[Fe^{III}T2MP]/M = 1.04 \times 10^{-5}$, $[Fe^{III}T3MP]/M = 1.17 \times 10^{-5}$; cell length 10 mm).

conducted. The absorbance of $Fe^{III}T2MP$ and $Fe^{III}T3MP$ over the concentration range of 5×10^{-7}–1.7×10^{-5} M at pH 1 and 13.4 was measured at several wavelengths (410, 412, and 430 nm for $Fe^{III}T2MP$, and 394, 417, and 432 nm for $Fe^{III}T3MP$). The excellent proportionality observed between the absorbance and [$Fe^{III}TMPs$] proved that the states of aggregation of the complexes do not change in this concentration region. Thus, the species at pH 1–4 and at 13.4 are perhaps both monomeric; the former may be a five-coordinated monoaqua complex as proposed for $Fe^{III}T4MP$.[2,5]

Consequently, the equilibrium between species at pH 1–4 and 8–10 may be presented by one of the following equations:

$$\text{monomer} \rightleftharpoons \text{monomer}' + n\text{H}^+ \quad (1)$$

$$2(\text{monomer}) \rightleftharpoons \text{dimer} + n\text{H}^+ \quad (2)$$

Table I gives the number of transferred protons, n, and the equilibrium constant, K_a, evaluated[8] from the data in Figure 3.

(8) (a) Fleisher, E. B.; Palmer, J. M.; Srivastava, T. S.; Chatterjee, A. *J. Am. Chem. Soc.* **1971**, *93*, 3162. (b) Pasternack, R. F.; Cobb, M. A. *J. Inorg. Nucl. Chem.* **1973**, *35*, 4327. (c) Pasternack, R. F.; Cobb, M. A.; Sutin, N. *Inorg. Chem.* **1975**, *14*, 866.

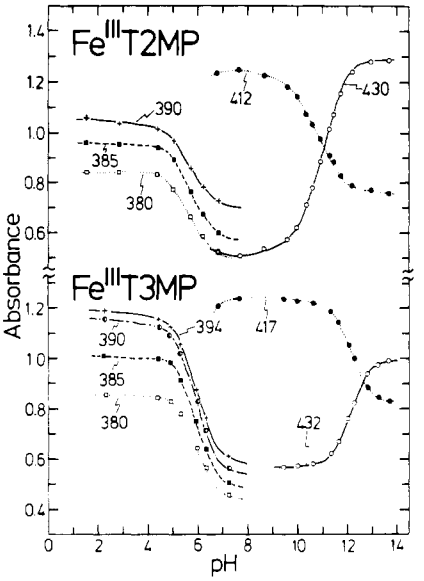

Figure 3. Spectrophotometric titration curves of $Fe^{III}T2MP$ and $Fe^{III}T3MP$ at several wavelengths, replotted from Figure 2. The numbers indicate the wavelengths.

Table I. Number of Transferred Protons (n) and Equilibrium Constants (K_a) Obtained from pH Titration Curves of $Fe^{III}TMP$[a]

		M ⇌ M′		2M ⇌ D	
$Fe^{III}TMP$	λ/nm	n	pK_a	n	pK_a
		pH 4–8			
$Fe^{III}T2MP$	390	0.83	4.8	1.20	8.1
	385	0.93	5.4	1.32	8.5
	380	1.00	5.8	1.30	8.4
		pH 9–13			
	412	0.88	9.6	1.35	14.0
	430	0.95	10.5	1.25	13.7
		pH 4–8			
$Fe^{III}T3MP$	394	0.90	5.5	1.30	8.1
	390	1.00	5.6	1.18	6.7
	385	1.08	6.4	1.62	10.5
	380	1.00	5.9	1.49	9.8
		pH 10–14			
	417	1.00	12.3	1.72	20.1
	432	1.00	12.2	1.71	19.9

[a] Abbreviations: M = monomer; M′ = monomer′; D = dimer.

Obviously, the equilibrium in the pH range of 4–8 involves the transfer of one proton between different monomers, since the n and pK_a values estimated by eq 1 are close to an integer and the pH value corresponding to the inflection point, respectively. The species between pH 8 and 10 may be presented as $Fe^{III}T2MP(OH)$ and $Fe^{III}T3MP(OH)$. Similarly, species at pH $\simeq$ 13 may be specified as $Fe^{III}T2MP(OH)_2$ and $Fe^{III}T3MP(OH)_2$; these dihydroxy-liganded complexes are strongly supported also by EPR data (see part iii). The pK_a values for $Fe^{III}T3MP$ and $Fe^{III}T4MP$ are similar and larger than the pK_a values of $Fe^{III}T2MP$.

(b) Proton Equilibria between $Fe^{II}TMP$ Species. Figure 4 shows the absorption spectra in the Soret region for the electrochemically reduced $Fe^{II}TMP$ species at various pH values. This figure includes also the dependence of the absorbance on pH at 426, 432, 439, and 446 nm. An equilibrium is recognized between species at pH 1–10 and 13–14. In the case of FeT4MP, it is known that electrochemically produced $Fe^{II}T4MP$ species are monomeric even if the initial $Fe^{III}T4MP$ solution contains dimeric species.[2] There is no such datum for FeT2MP or FeT3MP. However, since the n and pK_a values evaluated from eq 1 are relatively consistent with those obtained experimentally (Table II), FeT2MP and FeT3MP at pH 1–10 and 13–14 are also considered to be monomeric. The equilibrium between these species clearly consists of a one-proton

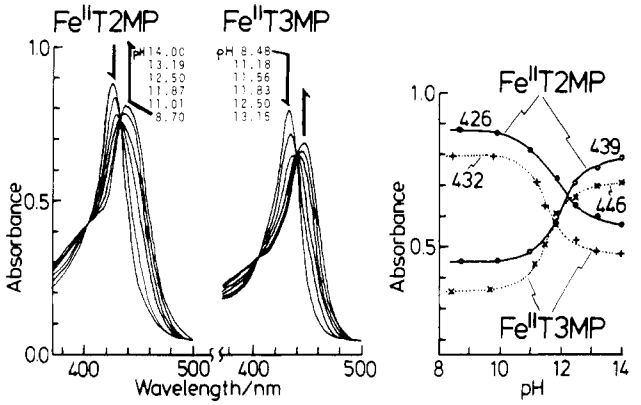

Figure 4. Soret absorption spectra of Fe^{II}T2MP and Fe^{II}T3MP aqueous solution at various pHs and pH dependence of absorbance at several wavelengths, replotted therefrom ([Fe^{III}T2MP]/M = 8.09 × 10^{-5}, [Fe^{III}T3MP]/M = 4.60 × 10^{-5}; cell length 1.04 mm; working electrode potential −0.7 V vs. SCE).

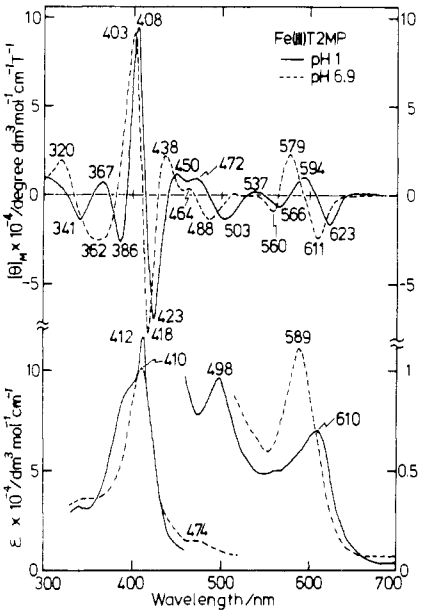

Figure 5. MCD (top) and absorption spectra (bottom) of Fe^{III}T2MP at pH 1 and 6.9 ([Fe^{III}T2MP]/M = 1.62 × 10^{-5} at pH 1 and 1.33 × 10^{-5} at pH 6.9). The cell length was 1 mm except for the visible region of absorption spectra (10 mm); the magnetic field was 1.1 T.

Table II. Number of Transferred Protons (n) and Equilibrium Constants (K_a) Obtained from pH Titration Curves of Fe^{II}TMP[a] (pH 10–13)

		M ⇌ M′		2M ⇌ D	
Fe^{II}TMP	λ/nm	n	pK_a	n	pK_a
Fe^{II}T2MP	426	0.85	10.4	1.30	13.6
	439	0.91	11.2	1.32	13.6
Fe^{II}T3MP	432	1.00	12.2	1.62	16.1
	446	1.00	12.2	1.67	16.5

[a] Abbreviations: M = monomer; M′ = monomer′; D = dimer.

transfer (Table II). pK_a values increase in the sequence Fe^{II}T4MP (11.2),[5] Fe^{II}T3MP (11.5), and Fe^{II}T2MP (11.9) in experiments under the same conditions.

(ii) Interpretation of Absorption and MCD Spectra. (a) Spectra of Fe^{III}TMP Species. The UV–visible absorption and MCD spectra at pH 1 and 7 for Fe^{III}T2MP and Fe^{III}T3MP are shown in Figures 5 and 6, respectively. As reported[5] for Fe^{III}T4MP, spectra at pH 1 are shifted to longer wavelengths (red shifted) from those at pH 7 (see especially the visible region and Figure 9), and less absorbance is seen in the former than the latter in the visible region. Although the shape of the visible absorption

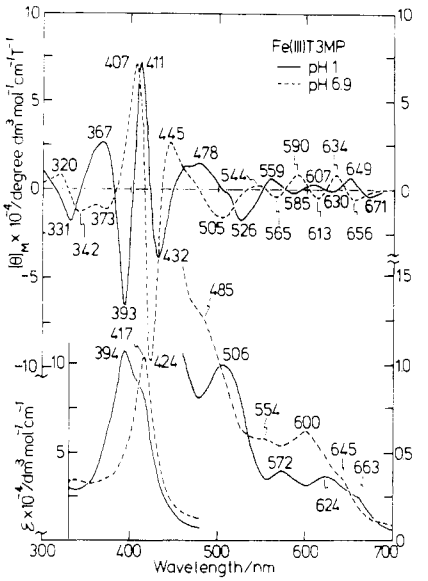

Figure 6. MCD (top) and absorption spectra (bottom) of Fe^{III}T3MP at pH 1 and 6.9 ([Fe^{III}T3MP]/M = 1.65 × 10^{-5} at pH 1 and 1.50 × 10^{-5} at pH 6.9). Other conditions are as for Figure 5.

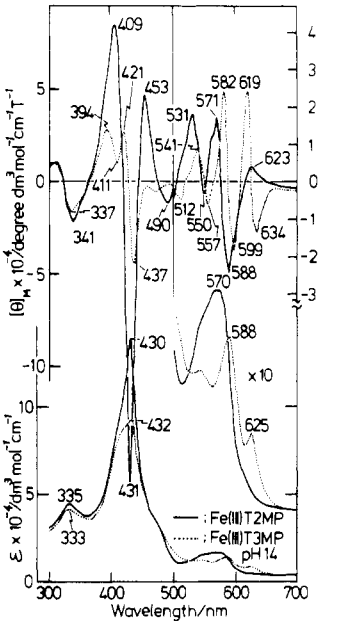

Figure 7. MCD (top) and absorption spectra (bottom) of Fe^{III}T2MP and Fe^{III}T3MP in 1 N NaOH ([Fe^{III}T2MP]/M = 1.33 × 10^{-5}, [Fe^{III}T3MP]/M = 1.50 × 10^{-5}). Other conditions are as for Figure 5.

bands of Fe^{III}T2MP differs from that of the typical high-spin-state complex such as (*meso*-tetraphenylporphinato)iron chloride, Fe^{III}TPP(Cl), these spectra, together with those of Fe^{III}T3MP, appear to belong to those of iron(III) high-spin grouping. The visible absorption spectrum of Fe^{III}T3MP at pH ca. 7 is that of the high-spin-state complex in shape.[9] In some of the spectra, the Soret MCD is very complicated. One reason for this complication is the superposition of blue-shifted Q_{0-0} MCD, which has a change in sign from minus to plus on the low-energy side. All MCD spectra are Faraday A-term type; i.e., dispersion type MCD spectra were observed corresponding to every absorption peak and shoulder.

The absorption and MCD spectra of Fe^{III}T2MP and Fe^{III}T3MP at pH 14 are shown in Figure 7. Compared with the spectra in Figures 5 and 6, the Soret band shifted to longer wavelengths, the Q band moved to shorter wavelengths, and the Soret MCD

(9) Kobayashi, H.; Shimizu, M.; Fujita, I. *Bull. Chem. Soc. Jpn.* **1970**, *43*, 2335.

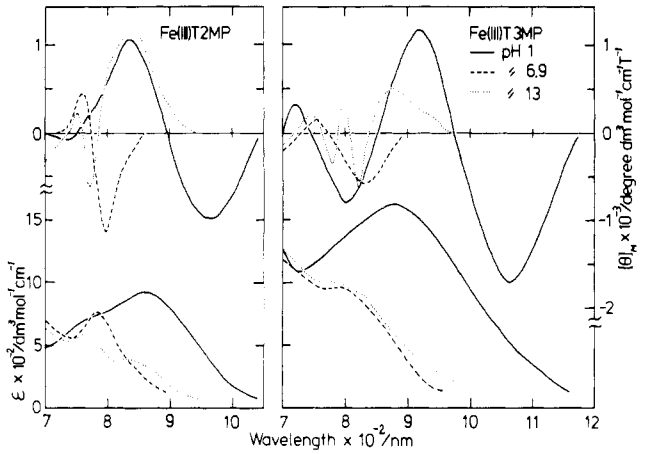

Figure 8. Near-IR MCD (top) and absorption spectra (bottom) of $Fe^{III}T2MP$ (left) and $Fe^{III}T3MP$ (right) ($[Fe^{III}T2MP]/M = 1.62 \times 10^{-4}$ at pH 1 and 1.71×10^{-5} at pH 6.9 and 13; $[Fe^{III}T3MP]/M = 0.83 \times 10^{-4}$ at pH 1 and 1.68×10^{-5} at pH 6.9 and 13; cell length 10 mm). MCD spectra are the average of several scans with use of a data processor (DP-500 attachement).

of $Fe^{III}T2MP$ was greatly intensified. These features are consistent with the general trend of an Fe^{III} high-to-low-spin transition.[10,11] As in Figures 5 and 6, the electronic and MCD spectra of $Fe^{III}T2MP$ were shifted to shorter wavelengths compared to the spectra of $Fe^{III}T3MP$, indicating that the difference in the position of the pyridinium group affects the porphyrin chromophore differently.

Figure 8 shows the MCD and absorption spectra in the near-IR region of $Fe^{III}T2MP$ and $Fe^{III}T3MP$. The bands of Fe^{III} porphyrins in this region have been assigned to a charge-transfer (CT) transition that is likely to be of the porphyrin-to-iron type.[11c,12] The MCD pattern corresponding to the longest wavelength absorption maxima which shows a change in sign from minus to plus from the longer wavelength side[13] indicates the species at pH 1 and 7 are Fe^{III} high-spin complexes. MCD spectra reveal the effective symmetry of iron in $Fe^{III}T2MP$ at pH 1 is approximately D_{4h} and the degeneracy in the E_g excited states is not appreciably removed. In contrast, the MCD curve of $Fe^{III}T3MP$ at pH 1 is nonsymmetrical probably due to the larger contribution of a Faraday C term,[13g] and its inflection points greatly deviate from the position of absorption maximum. Thus the effective symmetry of iron at pH 1 is higher in $Fe^{III}T2MP$ than in $Fe^{III}T3MP$. The symmetry of Fe^{III} at pH 7 appears to be lower than at pH 1 for both $Fe^{III}T2MP$ and $Fe^{III}T3MP$. Interestingly, the opposite relationship was observed for $Fe^{III}T4MP$; i.e., the effective symmetry of iron was higher for species at ca. pH 7 than at pH 1. Consequently, the effective symmetry of iron at pH 1 decreases in the order $Fe^{III}T2MP > Fe^{III}T4MP \simeq Fe^{III}T3MP$, while that at pH 7 decreases from $Fe^{III}T4MP$ to $Fe^{III}T2MP$ or $Fe^{III}T3MP$.

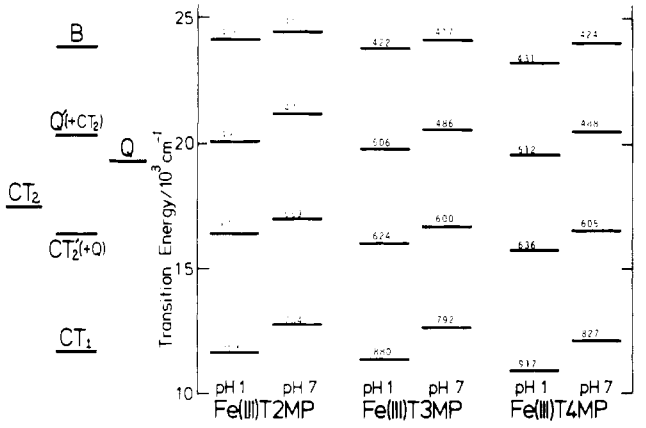

Figure 9. Band positions of $Fe^{III}TMPs$ at pH 1 and ca. 7, collected from either absorption or MCD spectra.

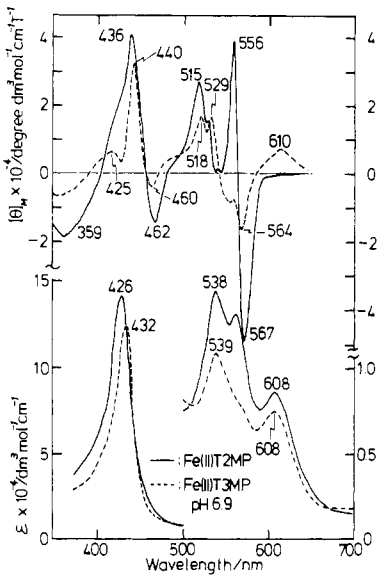

Figure 10. MCD (top) and absorption spectra (bottom) of $Fe^{III}T2MP$ and $Fe^{III}T3MP$ at pH 6.9. ($[Fe^{III}T2MP]/M = 8.09 \times 10^{-4}$, $[Fe^{III}T3MP]/M = 4.60 \times 10^{-5}$). Other conditions are as for Figure 4.

The MCD spectra at pH values above 13 show a change in sign from plus to minus on the longer wavelength side; this indicates low-spin Fe^{III} porphyrins.[13] The lowest energy positive MCD peak can be ascribed to the low-spin component.

In order to see whether there is any correlation between the band position and the position of the pyridinium group, the band positions of the $Fe^{III}TMP$ species at pH 1 and ca. 7, which could be judged from the absorption and/or MCD spectra, were plotted in Figure 9. For all $Fe^{III}TMPs$, the band positions at pH 7 apeared at shorter wavelengths than at pH 1 and the position of the MCD peak moved to longer wavelengths the farther the pyridinium group was from the porphyrin plane. Thus meso substituents contributed significantly to the porphyrin chromophore. Kobayashi et al.[14] discussed the MCD and absorption spectra of several Fe^{III} high-spin porphyrins. On the basis of calculation by the composite molecular orbital method Kobayashi concluded that the higher the (porphyrin-to-iron) CT state that interacts with the Soret state, the shorter the wavelength of the bands. In this study, it is concluded that the CT state is higher for species at pH 7 than at pH 1, and the CT state decreased in the order of $Fe^{III}T2MP$, $Fe^{III}T3MP$, and $Fe^{III}T4MP$. Results obtained in a spectroscopic study of hemoproteins indicate the higher the content of a high-spin component, the shorter the wavelengths of the visible and the near-IR CT.[11c] Therefore, it

(10) (a) Kobayashi, H.; Higuchi, T.; Eguchi, K. *Bull. Chem. Soc. Jpn.* **1976**, *49*, 457. (b) Vickery, L.; Nozawa, T.; Sauer, K. *J. Am. Chem. Soc.* **1976**, *98*, 343, 351. (c) Kobayashi, N.; Nozawa, T.; Hatano, M. *Biochim. Biophys. Acta* **1976**, *427*, 652.

(11) (a) Schoffa, G. *Adv. Chem. Phys.* **1964**, *7*, 182. (b) Yonetani, T. In "Probes of Structure and Function of Macromolecules and Membranes"; Chance, B., Yonetani, T., Mildvan, A. S., Eds.; Academic Press: New York and London, 1971; Vol. 2, 545. (c) Smith, D. W.; Williams, R. J. P. *Struct. Bonding (Berlin)* **1970**, *7*, 1.

(12) (a) Day, P.; Smith, D. W.; Williams, R. J. P. *Biochemistry* **1967**, *6*, 1563, 3747. (b) Zerner, M.; Gouterman, M.; Kobayashi, H. *Theor. Chim. Acta* **1966**, *6*, 363.

(13) (a) Cheng, J. C.; Osborne, G. A.; Stephens, P. J.; Eaton, W. A. *Nature (London)* **1973**, *241*, 193. (b) Stephens, P. J.; Sutherland, J. C.; Cheng, J. C.; Eaton, W. A. In "Proceedings of the International Conference on Excited States of Biological Molecules, Leiden"; Birks, J., Ed.; Wiley-Interscience: New York, 1976; p 434. (c) Nozawa, T.; Yamamoto, T.; Hatano, M. *Biochim. Biophys. Acta* **1976**, *427*, 28. (d) Kobayashi, N.; Nozawa, T.; Hatano, M. *Ibid.* **1977**, *493*, 340. (e) Nozawa, T.; Shimizu, T.; Hatano, M.; Shimada, H.; Iizuka, T.; Ishimura, Y. *Ibid.* **1978**, *534*, 285. (f) Kobayashi, N.; Nozawa, T.; Hatano, M. *Bull. Chem. Soc. Jpn.* **1981**, *54*, 919. (g) Yamamoto, T.; Nozawa, T.; Kobayashi, N. *Ibid.* **1982**, *55*, 3059.

(14) Kobayashi, H.; Kaizu, Y.; Tsuji, H. Abstracts, 45th Annual Meeting of the Chemical Society of Japan, Tokyo, April 1982, No. 2B36.

Table III. g Values for $Fe^{III}TMPs$ at Some pH Values[a]

	pH 1			pH 8.7			pH 13.7		
	$g_\perp$		$g_\parallel$	$g_\perp$		$g_\parallel$	g_x	g_y	g_z
$Fe^{III}TMP$	peak	trough	trough	peak	trough	trough	peak	midpoint	trough
FeT2MP	5.9782	5.1589	1.9402	6.6667	4.1953	1.9062	1.9137	2.1305	2.4481
FeT3MP	5.9718	5.1730	1.9545	6.2343	4.5572	1.9174	1.9045	2.1407	2.4732
FeT4MP	5.9419	5.1989	1.9710	5.9413	5.0325	1.9542	1.9044	2.1425	2.4711

[a] Concentrations of the sample solutions were ca. 1.0–3.2 mM.

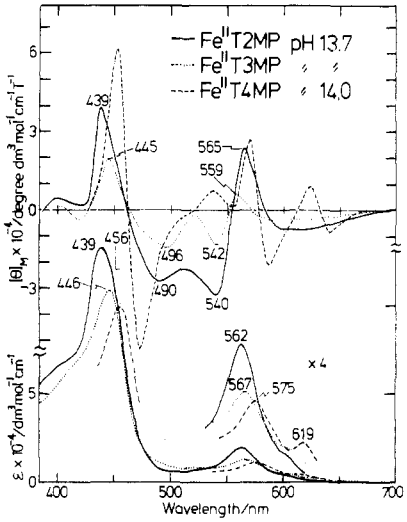

Figure 11. MCD (top) and absorption spectra (bottom) of $Fe^{II}TMPs$ at pH 13.7 or 14.0 ($[Fe^{III}T2MP]/M = 2.66 \times 10^{-5}$, $[Fe^{III}T3MP]/M = 3.16 \times 10^{-5}$). The spectra for $Fe^{II}T4MP$ were replotted from previous papers.[2a,5] Other conditions are as for Figure 4.

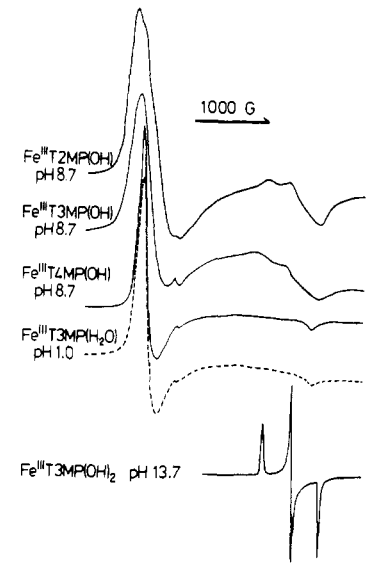

Figure 12. EPR spectra of $Fe^{III}TMPs$ at pH 8.7 and $Fe^{III}T3MP$ at pH 1 and 13.7 at 77 K ($[Fe^{III}TMPs]/M = 0.9–3.2$).

is concluded that the access of the pyridinium group to the porphyrin plane raised the content of the high-spin component. Although not shown, the energy differences among various bands (as B–CT_1, CT_2'–CT_1, Q′–CT_2, and CT_2'(pH 7)–CT_2'(pH 1)) do not depend markedly on the type of $Fe^{III}TMPs$.

The band positions of the species at pH values above 13 also shifted to shorter wavelengths on going from $Fe^{III}T4MP$ to $Fe^{III}T3MP$ to $Fe^{III}T2MP$; for example, the Soret bands appear at 440, 432, and 430 nm, Q_{0-0} bands at 633, 625, and 620 nm, and the MCD peak with the longest wavelength at 882, 877, and 843 nm for $Fe^{III}T4MP$, $Fe^{III}T3MP$, and $Fe^{III}T2MP$, respectively.

(b) Spectra of $Fe^{II}TMP$ Species. The MCD spectra of $Fe^{II}TMPs$ are nearly independent of pH from pH 1 to 10. The $Fe^{II}TMP$ species can be classified into the Fe^{II} high-spin grouping from the characteristic shape of the Soret band[10,15] (Figure 10). This species would have at least one axial ligand, since four-coordinate square-planar iron(II) tetraarylporphyrins have two bands of roughly equal intensity of opposite signs in the Soret region.[16] Since six-coordinate high-spin iron(II) porphyrins have not been reported to date, the species may be five-coordinated. The positions of the Soret absorption peaks shift from 445 nm[2a] for FeT4MP to 432 nm for FeT3MP and 426 nm for FeT2MP.

Figure 11 shows the MCD and absorption spectra of $Fe^{II}T2MP$, $Fe^{II}T3MP$, and $Fe^{II}T4MP$ at pH 13–14. In the case of $Fe^{II}T4MP$, the spectra were assigned to an Fe(II) low-spin complex[5] because substantially pure Faraday A terms were detected associated with the absorption maxima. Although we believe from the spectral similarity that the species are in a low-spin state, the A terms in this figure are deformed and their positions are not necessarily consistent with those of absorption peaks. This suggests a departure of the effective symmetry from D_{4h}. The possibility of a μ-oxo dimer may be ruled out by comparing the MCD spectrum with that of a reference compound, $(Fe^{II}TPP)_2O$, which produces a broad S-shaped curve easily distinguishable from the sharper bands of the normal porphyrin complexes.[17] Like the species at pH 1–10, the band positions of the Soret absorption peaks shifted to shorter wavelengths for $Fe^{II}T4MP$ (456 nm),[2a] $Fe^{II}T3MP$ (446 nm), and $Fe^{II}T2MP$ (439 nm). Thus the Soret band energy of the species at pH 13–14 is lower than that at pH 1–10 by ca. 540–730 cm^{-1}.

(iii) EPR Spectra. EPR spectra for the $Fe^{III}TMPs$ at pH ca. 8.7 are shown in Figure 12. The g values at pH 1 and 8.7 are given in Table III. The data in Table III indicates the species are all in high-spin states, in accord with the results in section a of part ii. However, in Figure 12 the sharp signal at $g \simeq 6$ for $Fe^{III}T4MP$ became broader in $Fe^{III}T3MP$ and finally split into two components for $Fe^{III}T2MP$. Also, the g value around 2 decreased concomitantly in this order. The g value in high-spin iron(III) accompanying a decrease in symmetry from tetragonal to rhombic can be expressed by eq 3 and 4 (D and E are zero-field

$$g_{x,y} = 6.01 \pm 24E/D - 18.7E^2/D^2 \quad (3)$$

$$g_z = 2.00 - 33.8E^2/D^2 \quad (4)$$

splitting parameters).[18] The above phenomenon indicates that the symmetry of the iron ion decreases from $Fe^{III}T4MP$ to $Fe^{III}T3MP$ and further to $Fe^{III}T2MP$. Although not so explicit, the situation is quite similar for species at pH 1. The spectra at this pH (shown only for $Fe^{III}T3MP$, broken line) are exemplary for Fe^{III} high-spin porphyrins with tetragonal symmetry. However, by careful experiments and analysis, it was found that $g_\perp$ values increase while $g_\parallel$ values decrease in the order of $Fe^{III}T4MP$, $Fe^{III}T3MP$, and $Fe^{III}T2MP$ (Table III) (note that when the

(15) Hatano, M.; Nozawa, T. *Adv. Biophys.* **1978**, *11*, 95.
(16) Collman, J. P.; Brauman, J. I.; Doxsee, K. M.; Halbert, T. R.; Bunnenberg, E.; Rinder, R. E.; LaMar, B. N.; Gaudio, J. D.; Lang, G.; Spartalian, K. *J. Am. Chem. Soc.* **1980**, *102*, 4182.
(17) Collman, J. P.; Basolo, F.; Bunnenberg, E.; Collins, T. J.; Dawson, J. H.; Ellis, P. E., Jr.; Marrocco, M. L.; Moscowitz, A.; Sessler, J. L.; Szymanski, T. *J. Am. Chem. Soc.* **1981**, *103*, 5636.
(18) (a) Palmer, G. In "The Porphyrins"; Dolphin, D., Ed.; Academic Press: New York and London, 1979; Vol. 4, Chapter 6. (b) Kotani, M.; Watari, H. In "Magnetic Resonance in Biological Research"; Franconi, C., Ed.; Gordon and Breach: New York, London, and Paris, 1971; p 75.

Table IV. g Values, Coefficients of the Basis Function, and Ligand Field Parameters for $Fe^{III}TMPs$ at pH 13.7

	principal g values			coeffs of basis function			tetragonal	rhombic	rhombicity
$Fe^{III}TMP$	g_x	g_y	g_z	a	b	c	splitting μ in λ[a]	splitting R in λ[a]	R/μ
FeT2MP	1.9137	2.1305	2.4481	0.9916	0.1157	0.0470	9.5078	4.4047	0.4633
FeT3MP	1.9045	2.1407	2.4732	0.9910	0.1222	0.0508	8.7926	4.1732	0.4746
FeT4MP	1.9044	2.1425	2.4711	0.9910	0.1217	0.0511	8.6946	4.1934	0.4823

[a] λ is the spin–orbit coupling constant.

Scheme I

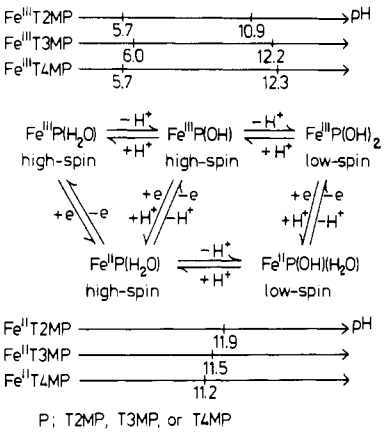

Scheme II

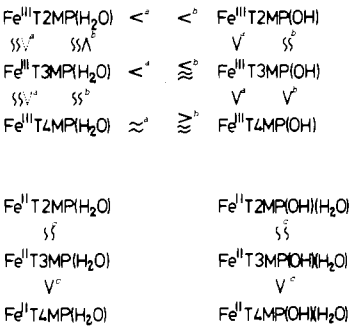

[a] As deduced from EPR data. [b] As deduced from near-IR MCD data. [c] As deduced from UV-visible MCD data.

splitting between g_x and g_y is very small, the g value obtained at the peak of $g \simeq 6$ signal reflects mainly the g_x value; so if the rhombicity becomes large, the g value also becomes large). For $Fe^{III}T2MP$ and $Fe^{III}T3MP$, a rhombic distortion is smaller at pH 1–4 than at 7–9. Since the increase of rhombic distortion in high-spin iron(III) has been recognized by a change from $Fe^{III}TPP(Cl)$ to $Fe^{III}TPP(OMe)$,[19] the species at pH 7–9 may have an axial ligand with stronger ligand field strength.

The EPR spectrum for $Fe^{III}T3MP$ at pH 13.7 is also shown in Figure 12. $Fe^{III}T2MP$ and $Fe^{III}T4MP$ reveal similar spectra at this pH but are not shown. These species are in the low-spin ground states. The g values were analyzed with the assumption of a pure t_2^5 electron configuration, and the obtained crystal field parameters are given in Table IV.[20] There are six types of axial ligation modes reported in the literature.[21] The tetragonal splitting μ had the same magnitude as the largest of the six types reported and increased in the sequence $Fe^{III}T4MP < Fe^{III}T3MP < Fe^{III}T2MP$. The rhombic splitting R is the largest for $Fe^{III}T2MP$ and the rhombicity, R/μ, decreases in the above order. The values of R/μ obtained ($0.463 < R/\mu < 0.483$) are very close to 0.501, which is the R/μ value of iron(III) low-spin porphyrins with an axial ligation mode of O–Fe–O[19] and therefore strongly suggests that the species at this pH should be formulated as $Fe^{III}TMP(OH)_2$. If both the fifth and sixth axial positions are occupied by H_2O, the species would be in the high-spin state[22] because of its weak σ-donor strength.[23] The tetragonal splitting depends primarily on the charge of the iron atom, and this in turn is determined by the sum of the σ- and π-donor strengths of the ligands.[24] As mentioned above, the axial ligation positions of FeTMPs appear to be occupied solely by two OH^- ions. The μ values in Table IV suggest the sum of the ligand field of porphyrin nitrogens becomes stronger the closer the pyridinium group is to the porphyrin plane. Thus, even though the pyridinium group does not reside within the porphyrin plane, it does affect ligand field strength.

Concluding Remarks

The major monomeric species in water and their spin states as deduced from the present study are shown in Scheme I.[25] Three ferric and two ferrous species are sufficient to explain the results between pH 1 and 14. Proton equilibria exist between the three $Fe^{III}TMP$ monomers with pK_a values around 5–6 and 11–12. Proton equilibria also exist between the iron(II) porphyrin species with pK_a values around 11–12.

Scheme II (upper half) represents the relative degree of rhombic distortion or the reduction of effective symmetry of iron among several high-spin iron(III) species as deduced from EPR and near-IR MCD data. Although there are some deviations in the results between EPR and MCD, it may be concluded that the effective symmetry of iron is lower for species coordinated by strong ligand field ligands ($Fe^{III}TMP(OH)$ rather than $Fe^{III}TMP(H_2O)$) and for those whose pyridinium groups are situated closer to the porphyrin plane ($Fe^{III}T2MP(OH)$ rather than $Fe^{III}T4MP(OH)$). The lower half of this scheme shows the results for ferrous species as judged by MCD. The symmetry of iron in $Fe^{II}T4MP$ appears to be higher than that in $Fe^{II}T2MP$ and $Fe^{II}T3MP$.

Other main results of the present study are summarized as follows: (i) among $Fe^{III}TMP(OH)_2$s, tetragonal splitting increases while rhombicity decreases from $Fe^{III}T4MP$ to $Fe^{III}T3MP$ and further to $Fe^{III}T2MP$; (ii) the CT state for $Fe^{III}TMP(OH)$s is higher than for $Fe^{III}TMP(H_2O)$s both in the visible (transition from $b_{2u}(\pi)$ and $a_{2u}(\pi)$ to $e_g(d\pi)$ in a D_{4h} notation) and in the near-IR ($a_{1u}(\pi)$ and $a_{2u}(\pi)$ to $e_g(d\pi)$) regions[11c,12,13c,g] and it heightens in the order of $Fe^{III}T4MP$, $Fe^{III}T3MP$, and $Fe^{III}T2MP$.

Acknowledgment. I am grateful to Dr. T. Kuwana for the donation of FeTMP samples, Dr. H. Yokoi for his courtesy in measuring EPR spectra, and Professor Y. Nishiyama for his encouragement throughout this work. This work was partially supported by a Grant-in-Aid for Scientific Research from the Ministry of Education, Science and Culture (No. 59750698).

Registry No. $Fe^{III}T2MP$, 97878-20-1; $Fe^{III}T3MP$, 94288-76-3; $Fe^{III}T4MP$, 60489-13-6; $Fe^{II}T2MP$, 97878-21-2; $Fe^{II}T3MP$, 97878-22-3; $Fe^{II}T4MP$, 71794-64-4; $Fe^{III}T2MP(H_2O)$, 97878-23-4; $Fe^{III}T3MP$-

(19) Otsuka, T.; Ohya, T.; Sato, M. *Inorg. Chem.* **1984**, *23*, 1777.
(20) (a) Stephens, K. W. H. *Proc. R. Soc. London, Ser. A* **1953**, *219*, 542. (b) Salmeen, I.; Palmer, G. *J. Phys. Chem.* **1968**, *48* 2049. (c) Sato, M.; Ohya, T.; Morishima, I. *Mol. Phys.* **1981**, *42*, 475.
(21) (a) Tang, S. C.; Koch, S.; Papaefthymiou, G. C.; Foner, S.; Frankel, R. B.; Ibers, J. A.; Holm, R. H. *J. Am. Chem. Soc.* **1976**, *98*, 2414. (b) Blumberg, W. E.; Peisach, J. In "Probes of Structure and Function of Macromolecules and Membranes"; Chance, T., Yonetani, T., Mildvan, A. S., Eds.; Academic Press: New York, 1971; Vol. 2, p 215.
(22) Kastner, M. E.; Scheidt, W. R.; Mashiko, T.; Reed, C. A. *J. Am. Chem. Soc.* **1978**, *100*, 666.
(23) Houghton, R. P. "Metal Complexes in Organic Chemistry"; Cambridge University Press: New York, 1979.
(24) Blumberg, W. E.; Peisach, J. In ref 18b, p 67.
(25) In drawing this scheme, we confirmed separately that electroreduction of $Fe^{III}TMP(OH)$ and $Fe^{III}TMP(OH)_2$ consumes a proton as reported for the corresponding species of $Fe^{III}T4MP$.[2b]

(H_2O), 97878-24-5; $Fe^{III}T4MP(H_2O)$, 65774-47-2; $Fe^{III}T2MP(OH)$, 97889-69-5; $Fe^{III}T3MP(OH)$, 97878-25-6; $Fe^{III}T4MP(OH)$, 97889-58-2; $Fe^{III}T2MP(OH)_2$, 97878-26-7; $Fe^{III}T3MP(OH)_2$, 97889-59-3; $Fe^{III}T4MP(OH)_2$, 75908-34-8; $Fe^{II}T2MP(H_2O)$, 97878-27-8; $Fe^{II}T3MP(H_2O)$, 97878-28-9; $Fe^{II}T4MP(H_2O)$, 97878-29-0; $Fe^{II}T2MP(OH)(H_2O)$, 97878-30-3; $Fe^{II}T3MP(OH)(H_2O)$, 97878-31-4; $Fe^{II}T4MP(OH)(H_2O)$, 75908-36-0; $Fe^{III}T2MP(Cl)$, 97878-32-5; $Fe^{III}T3MP(Cl)$, 97878-33-6.

Contribution from the Chemistry Department, University of Stirling, Stirling FK9 4LA, Scotland, and Department of Chemistry, University of Florence, 50132 Firenze, Italy

Noncyclic Reference Ligands for Tetraaza Macrocycles. Synthesis and Thermodynamic Properties of a Series of α,ω-Di-N-methylated Tetraaza Ligands and Their Copper(II) Complexes

ROBERT M. CLAY,*[1] STUART CORR,[1] MAURO MICHELONI,[2] and PIERO PAOLETTI[2]

Received August 1, 1984

The synthesis and characterization of 2,5,8,11-tetraazadodecane, 2,5,9,12-tetraazatridecane, 2,6,9,13-tetraazatetradecane, and 2,6,10,14-tetraazapentadecane are described. The protonation constants (pK_{1-4}) for these ligands have been determined together with the stepwise enthalpies of protonation (ΔH_{1-4}). ^{13}C NMR provides evidence for the sequence of protonation of the four nitrogen atoms. K_{ML} and ΔH° values for the formation of the copper(II) complexes have been determined, and it has been shown that the behavior of this series of di-N-methylated ligands toward both protonation and copper(II) complex formation parallels that of the simple tetraaza macrocyclic ligands much more closely than that of noncyclic reference ligands containing terminal primary amine groups. With regard to the macrocyclic effect, both free energy and enthalpy terms are essentially independent of the size of the ligands.

Introduction

Considerable interest has been shown in recent years in the thermodynamic origins of the macrocyclic effect, the term used to describe the enhanced stability of the metal complexes of a macrocyclic ligand over similar complexes of an analogous noncyclic ligand.[3] Early work ascribed the macrocyclic effect exclusively to either enthalpy[4] or entropy[5,6] terms, although more recently, by use of direct calorimetric values of enthalpy,[7,10] it has been shown, at least for tetraaza ligands, that the entropy term is always favorable whereas the enthalpy term varies in magnitude with the matching of size of the metal ion and the aperture in the macrocyclic ligand. In assessing the magnitude of the macrocyclic effect, represented by the metathetic reaction

$$[ML_{noncyclic}]^{n+}(aq) + L_{cyclic}(aq) \rightarrow [ML_{cyclic}]^{n+}(aq) + L_{noncyclic}(aq)$$

it is necessary, for any particular macrocyclic ligand, to choose a suitable noncyclic reference. Traditionally, when considering tetraaza macrocyclic ligands in series I (see Chart I), different authors have used a noncyclic ligand from series II and have tried to ensure that the sequencing of the chelate rings is the same. Thus the thermodynamic properties of complexes of L_1 have been compared to those of L_6[8] (all chelate rings being five-membered) whereas the properties of complexes of L_3 have been compared to those of L_7[4] (the alternating sequence of five- and six-membered rings remains the same). This choice of reference ligand has had the added advantage that the ligands themselves were readily available and the thermodynamic properties of their metal complexes had already been determined.

Chart I

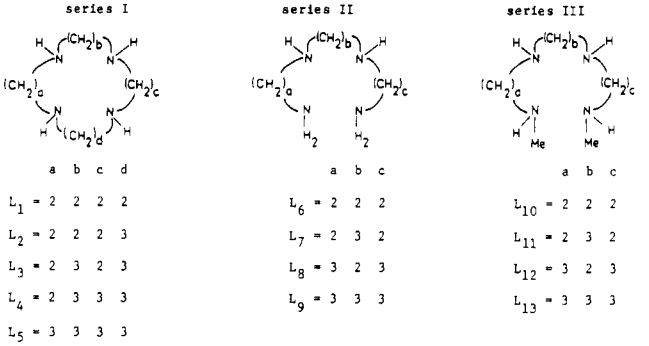

A more critical appraisal, however, suggests that ligands from series II may not be the most appropriate choice for two reasons.[11] First, the macrocyclic ligands contain four secondary amine nitrogen donor atoms compared with two secondary and two primary amine nitrogens for the reference ligands. It has already been established for complexes with N-alkylated ethylenediamines that changing a primary amine nitrogen to a secondary by, e.g., N-methylation causes a significant change in both ΔG°[12] and ΔH°.[13] Second, the macrocyclic enthalpy term (ΔH_{mac}) is made up of three component terms, as shown in the thermochemical cycle of Scheme I. The second of these terms is the difference in solvation enthalpies of the two complexes and is virtually impossible to determine experimentally.[14] In an experimental investigation into the contribution that the solvation of the free ligands makes to the macrocyclic enthalpy, it is, therefore, very desirable to minimize any difference between the hydration enthalpies of the two complexes.[15] Enthalpies of hydration are dependent on both ionic

(1) University of Stirling.
(2) University of Florence.
(3) Cabbiness, D. K.; Margerum, D. W. *J. Am. Chem. Soc.* **1969**, *91*, 6540.
(4) Hinz, F. P.; Margerum, D. W. *Inorg. Chem.* **1974**, *13*, 2941.
(5) Kodama, M.; Kimura, E. *J. Chem. Soc., Chem. Commun.* **1975**, 326.
(6) Kodama, M.; Kimura, E. *J. Chem. Soc., Dalton Trans.* **1976**, *116*, 2341.
(7) Anichini, A.; Fabbrizzi, L.; Paoletti, P.; Clay, R. M. *J. Chem. Soc., Chem. Commun.* **1977**, 244.
(8) Anichini, A.; Fabbrizzi, L.; Paoletti, P.; Clay, R. M. *J. Chem. Soc., Dalton Trans.* **1978**, 577.
(9) Fabbrizzi, L.; Micheloni, M.; Paoletti, P. *J. Chem. Soc., Dalton Trans.* **1979**, 1581.
(10) Gallori, E.; Martini, E.; Micheloni, M.; Paoletti, P. *J. Chem. Soc., Dalton Trans.* **1980**, 1722.
(11) Clay, R. M.; McCormac, H.; Micheloni, M.; Paoletti, P. *Inorg. Chem.* **1982**, *21*, 2494.
(12) Smiith, R. M.; Martell, A. E. "Critical Stability Constants"; Plenum Press: New York, 1975; Vol. 2.
(13) Paoletti, P.; Fabbrizzi, L.; Barbucci, R. *Inorg. Chim. Acta, Rev.* **1973**, *7*, 43.
(14) Clay, R. M.; Micheloni, M.; Paoletti, P.; Steele, W. V. *J. Am. Chem. Soc.* **1979**, *101*, 4419.

0020-1669/85/1324-3330$01.50/0